Sys Rev Pharm 2020;11(6):1188-1195
A multifaceted review journal in the field of pharmacy

Simple chemical synthesis of zinc oxide and copper oxide nanoparticles for biological protection

Nibras Abdul-Ameer Aboud [1]. Wafaa M.S Alkayat[2]. Dhia H Hussain[3]

[1]Department of Chemical Industrial, Institute of Technology/ Baghdad, Middle Technical University, Iraq.
[2]PhysicsDepartment, College of science, Mustansiriyah University, Baghdad, Iraq
[3]Chemistry Department, College of science, Mustansiriyah University, Baghdad, Iraq
*Corresponding author: nibrasabdulameer@gmail.com

ABSTRACT

In this study, Nanoparticle synthesized zinc oxide (ZnO) and copper oxide (CuO) in (PVP) polyvinylpyrrolidone as a dispersing agent with a simple chemical reaction used for the antimicrobial activity. Various concentrations of metal oxide with PVP synthesis as (0.02, 0.05, 0.1, and 0.4) M. The result of the x-ray diffraction indicated the presence of pure-phase ZnO and CuO with hexagonal and monoclinical structures with average crystal sizes(20.18), (32.89), (43.42) and (49.51) while the values (13.56), (23.94), (25.60) and (26.92) nm for ZnO and CuO respectively. Transmission electron microscopy analysis has shown that the average grain size of these nanoparticles increased with increasing concentrations (40-80) for ZnO and (35-50) nm for CuO. Energy dispersive analysis of x-rays clearly confirmed the presence of Zn, Cu, and O at a 1:1 atomic ratio while the particle sizes obtain from Atomic force microscopy (AFM) were (31.63-84.80) for ZnO, (32.34-60.23) nm for CuO with [0.02- 0.4] M ZnO and CuO nanoparticles in suspension showed activity against a range of bacterial pathogens as (Staph. Aurous, Staph. Epidermidis), gram-negative bacteria as (E. coli, Klebsiella spp.) and fungi (such as Candida albicans) with different concentrations, as comparing The extent of the inhibition zones between two oxides found to be concentration-dependent, These have been observed that ZnO nanoparticles have an extremely good bactericidal potential the Inhibition Zone demonstrates 30 mm in dishes with 0.4 M for Staphylococcus epidermidis as a positive gram. Although CuO nanoparticles have less bactericidal capacity in the Inhibition Region relative to ZnO and the maximum potential CuO has been shown to be positive gram in 25 mm with 0.4 M for Staphylococcus aurus.

Keywords: ZnO, CuO, PVP, AFM, SEM, antibacterial agent.

Correspondence:
Nibras Abdul-Ameer Aboud [1]
[1]Department of Chemical Industrial, Institute of Technology/ Baghdad, Middle Technical University, Iraq.
E-mail nibrasabdulameer@gmail.com

INTRODUCTION

The development of infectious diseases generally poses a risk to public health worldwide, especially with the creation of bacterial strains resistant to antibiotics. Both Gram-positive and Gram-negative bacterial strains are generally thought to present a main public health problem. Antibiotics have been used over the years to treat community-and hospital-derived infections (1,2).

Nanotechnology is the research that makes it possible to create new nano-materials within a nanoscale of less than 100 nm. This is commonly used in all areas due to the special and distinctive physical and chemical properties of nano materials (3-13). Current Nano biotechnological developments, particularly the ability to prepare metal oxide nanomaterials of specific size and shape, are likely to lead to the development of new antibacterial agents(14).

The particle size is primarily determined by the practical behavior of nanoparticles. Therefore, owing to their unusual chemical and physical properties, nanoparticles gained considerable interest (15,16). It is easy to modify the properties of nanoparticles by reducing or modifying their size, particularly when the nanometer scale manipulations are finished. In light of these special properties, Nano sized organic and inorganic particles are produced for ultimate use in medicinal products such as ZnO and CuO (17,18). Bacterial cell size is usually in the micrometer range while its outer cell membranes already have pores in just the nanometer scale. Since nanoparticles could be small in size than bacterial and fungal pores, they can cross the cell membrane in a specific manner and damage the cell (19). Metal nanoparticles easily diffuse through a successful wall of bacteria to connect to internal proteins and organelles, which lead to death of the bacteria. While some surfactants enhance cell growth, others hinder cell growth and may cause death of cells. The synthesis of nanoparticles with certain surfactants will have the effect of encouraging or hindering cell proliferation respectively (20).

The use of inorganic antimicrobials in pollution control has been highlighted as they provide important points which correspond to natural antimicrobials, for example, reduced host damage, more stable microbial opposition, high selectivity (21).

Metal oxide nanoparticles are widely considered by inorganic nanoparticles for their antibacterial activities. This is mostly because metal oxides have simple synthesis routes that can be managed to change the nanoparticles size and shape, and they are relatively cheap compared to metal nanoparticles like silver and gold. Zinc and Copper oxides are considered acceptable replacements to organic antimicrobials (22).

Experimental Section

1-Synthesis of ZnO nanostructure

ZnO Nanoparticles were prepared by the simple chemical reaction of zinc salts at 100 ° C, typically (0.02, 0.05, 0.1 and 0.4) M of Zinc nitrate hexahydrate Zn $(NO_3)_2{\cdot}6H_2O$. (BDH Chemicals Ltd Pool England) was dissolved in 50 ml deionized water in round bottom flask ,the solution was stirred at 450 rpm for 15 min then added to 1 wt.% (PVP) (C_6H_9NO) n [MW = 58,000 g mol^{-1}]Used as a surfactant agent, dissolved in 25 ml of deionized water at room temperature. Next, NaOH was added to the above solution in a 1: 2 ratio of highly stirred at 1500 rpm with an increased reaction temperature consisting of the nano suspension, the suspension stirred continuously at a constant speed for 3 hours. White precipitate appeared

indicating the formation of ZnO, after cooling to room temperature the precipitate was centrifuged, separated and several times washed with deionized water and ethanol. Finally, the precipitate was dried in an oven at 120 ˚ C for 1h and calcination at 400 ˚ C for 3h.

2- Synthesis of CuO nanostructure

While For CuO preparations with concentration (0.02 ,0. 05, 0.1 ,0.4) M, used starting material Copper (II) Nitrate Trihydrate $Cu(NO_3)_2.3H_2O$ (BDH Chemicals Ltd Pool England) dissolved in 50 ml Deionized water (DI) , the solution stirred at 450 rpm for 10 min. 1 wt.% PVP dissolved in 25 ml deionized water at room temperature was added then NaOH dropwise added With 1: 2- mole ratio at vigorous stirring with 1500 rpm with increase in reaction temperature to 70 ˚ C then the solution was continuously stirred at a constant speed for 2h. When a suspension was formed. The color change to dark blue, the precipitate was separated by centrifuge then washed several times with deionized water and ethanol, then dried in an oven at 80º C to remove moisture and calcination at 250C˚ for 3h black precipitate formed.

Results and Discussion

1- UV–Visible

By using UV – Visible spectrophotometer (SHIMADZU UV-Vis 160v) within the range of 200–900 nm, the optical properties of ZnO and CuO have been identified in Fig. (1) Displays the zinc oxide and copper oxide UV absorption spectra at room temperature. In 0.1 M ZnO spectra, an expansive top at 345 nm related to the ZnO excitation band was observed while for 0.02 M CuO nanoparticles excitation band at 750 nm. The tauc plots were used to calculate Photon Energy from ZnO and CuO wavelength.

$(\alpha hv)^{1/n} = A\,(hv - Eg)$ ..... (1)

Where α is the absorption coefficient, h is the Planck's constant, ν is the photon's frequency, Eg is the band gap and A is a proportionality constant, the exponent value indicates the nature of Electronic transmission, forbidden or allowed, direct or indirect: so for the direct allowed transitions n=1/2. The planning $(\alpha h \nu)^{1/n}$ versus (h ν) is a test issue of n = 1/2 for an examination that gives a superior fit, as utilized in search (23). The energy band gap of ZnO nanoparticles was estimated by plotting $(\alpha hv)^2$ versus (hv) as shown in fig. (1). The value of the optical band gap of ZnO is about 3.6 eV These results are compatible with research findings (24).The value of the optical band gap of CuO NPs is about (1.6) eV there was good agreement with the value of the energy published in the literature (25).

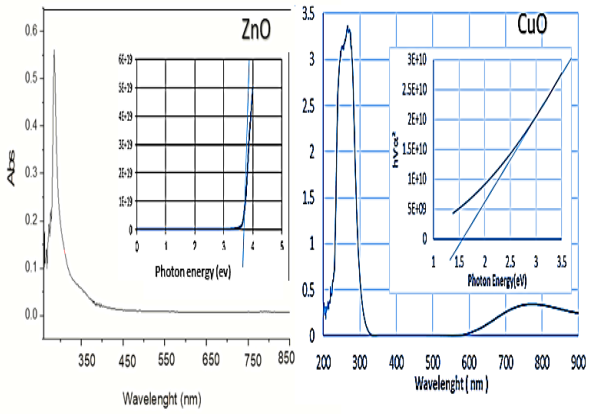

Figure 1. UV-Vis and energy gap of two the metal oxides

2- X-ray diffraction analysis

The nanostructure (zinc oxide and copper oxide) were explored by x-ray diffraction type (SHIMADZU XRD-6000). The XRD utilizing CuKα radiation line of 1.54 A˚ wavelength with 2θ run (10˚-80˚) .The XRD analysis for ZnO showed all samples with different concentrations would be perfectly indexed as being hexagonal wurtzite structure as compared with ZnO (JCPDS NO.36-1451) without any impurity as compared with data get in the literature (26). That the diffraction peaks were sharp and with different intensity, the 2θ (deg) for ZnO 0.02 M is shown in fig. (2) appeared in 31.79˚, 34.44 ˚, 36.27 ˚, 47.16 ˚, 56.62 ˚, 62.88 ˚, 66.39 ˚, 67.98 ˚ and 69.10 ˚ corresponding reflecting planes are (100), (002), (101), (102), (110), (103), (200), (112) and (201) respectively. While the ZnO XRD pattern for ZnO 0.05, 0.1 and 0.4 show the same orientations, but at very little offsets in 2θ (deg).

Likewise, the average crystallite sizes (D) were determined by utilizing the Debye-Scherer equation.

$D = (K\lambda)/(B \cos\theta)$ ---------- (2)

K is a consistent equivalent to 0.9; λ is wavelength of Cu Kα radiation,

B is the Full width half maximum of the diffraction peak expressed in theta then converted to radians and θ is the Bragg angles of the main planes.

The average size of crystallites Estimated by applying the Debye-Scherer equation was about

(20.18) - (49.51) nm for (0.02- 0.4) M of ZnO Table (1) illustrate the D with concentration. A broadening diffraction peaks of the crystalline pattern and reduced particle size Revealed that nano

synthesis has a good product and These results are consistent with the results published in the research(27).

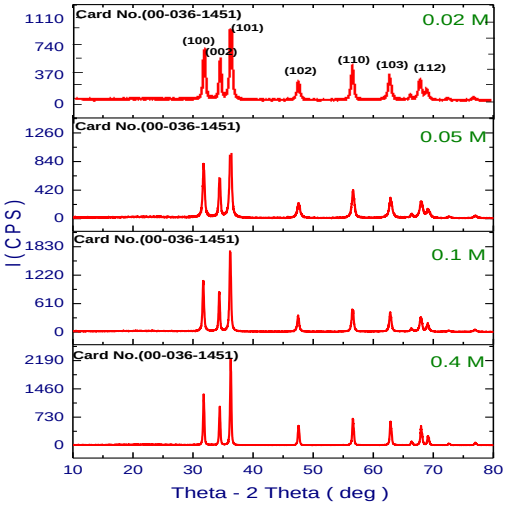

Figure 2. XRD pattern of ZnO with different concentration.

Concentration	0.02M	0.05M	0.1M	0.4M
average crystallites size (D) nm	20.18	32.89	43.42	49.51

Table (1) concentration and average crystalline size of ZnO

The XRD of CuO patterns show that all of the diffraction peaks are in good agreement with the standard diffraction data for CuO (JCPDS NO.48-1548), no characteristic peaks were observed for other oxides (such as Cu_2O or Cu_2O_3) This was also explained by the researcher in reference(28). The 2θ (deg) for CuO is shown in fig. (3) The diffraction peaks for 0.02 M Show the most brooding pattern at 32.42˚, 35.50˚, 38.71˚, 48.84˚, 58.31˚, 61.56 ˚, 66.32˚ and 67.90 ˚ corresponding reflecting planes are (110), (002), (200), (20-2), (202) (11-3), (31-1) and (113) respectively. As for the rest of the (0.05, 0.1, 0.4 M), the copper nanoparticles were given identical peaks with the card, but with very little displacement, as shown by the values and transitions on the pattern.

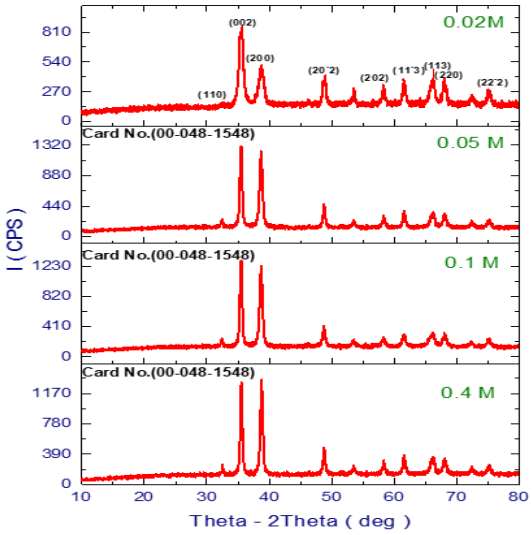

Figure 3. XRD pattern of CuO with different concentration.

The average sample crystallite sizes (D) were determined using the Debye-Scherer equation (2) for (0.02, 0.05, 0.1and 0.4) M CuO, respectively, tabled in table (2)

Table 2. Concentration and average crystalline size of CuO

Concentration	0.02M	0.05M	0.1M	0.4M
average crystallites size (D) nm	13.56	23.94	25.60	26.92

3- AFM and SEM analysis

Coated surface morphology were described by using the atomic force microscopy (model AA3000, Angstrom Advanced Inc., USA). The nanostructure (ZnO and CuO) has a hemispherical shape with perfect and vertically comparable grains. Evaluated grain size and mean square roughness were determined and listed in the tables (3-4). The results of the AFM analysis of ZnO showed this homogeneity of the surface. It is seen that the grain characters of the samples increase with increasing molarity, causing the different in roughness and in the square root probably due to the diffusion mechanism. 0.02 M ZnO showed with average grain size 31.63 nm while the average grain size of 0.4 M ZnO is 84.80 nm, grain Size, roughness and root mean square (rms)of ZnO shown in the table (3).

Table 3. Grain Size, roughness and root mean square of ZnO

No.	Molarities (M)	Grain Size(nm)	Roughness Density (nm)	Root Mean Square (nm)
1-	0.02	31.63	6.47	7.57
2-	0.05	70.18	4.2	4.94
3-	0.1	79.01	9.75	11.3
4	0.4	84.80	5.32	6.03

In addition, 3D image fig. (4, a) show histograms of the ZnO nanoparticles, illustrate that the different in homogeneity of the surface with different concentration. From Granularity accumulation distribution chart. Fig. (4, b) ZnO show the lowest and highest value of the granular volume was ranging from (22-55), (45-82), (43-140) and (42-100) nm for 0.02, 0.05, 0.1 and 0.4 M respectively, the surface morphology of the oxide, as seen in Fig. (4), indicates that the grains were evenly dispersed. The grain size increases with the molar concentration when increased the presence of high nanoscale sizes be close to 100 nanometers.

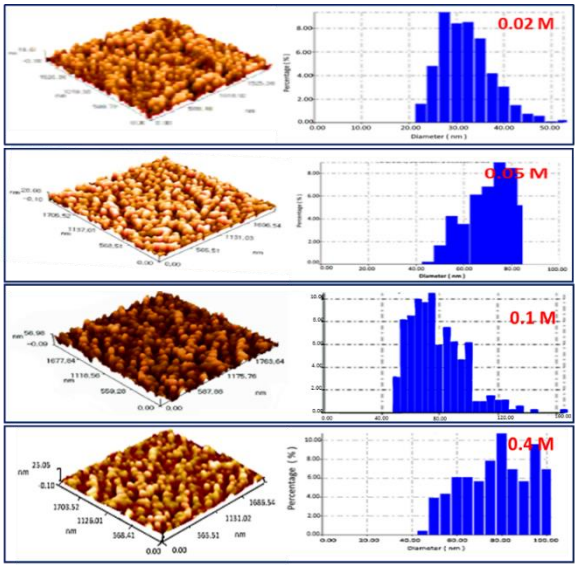

Figure 4. The AFM of ZnO

CuO surface morphology showed roughness , root mean square(rms) and grain size Explained in the table (4) , average grain size for 0.02 M CuO is 32.34 nm while for 0.4 M CuO is 60.23 nm .

Table 4. Grain Size, roughness and root mean square of CuO

	Molarities (M)	Grain Size(nm)	Roughness Density (nm)	Root Mean Square (nm)
1-	0.02	32.34	3.87	4.6
2-	0.05	43.2	1.13	2.41
3-	0.1	47.01	8.20	9.41
4	0.4	60.23	8.31	9.8

Fig. (5, a) 3D image of the CuO nanoparticles shows that the grains are distributed between (25-45), (5 -50), (20 - 70) and (47-80) nm for 0.02, 0.05, 0.1 and 0.4 M respectively

From 3D image , histograms for CuO exhibits that the particle size in nanoscale with relative increase in grain size although increase in molar concentration that due to present of PVP as surfactant agent that prevent the particle aggregation (29,30).

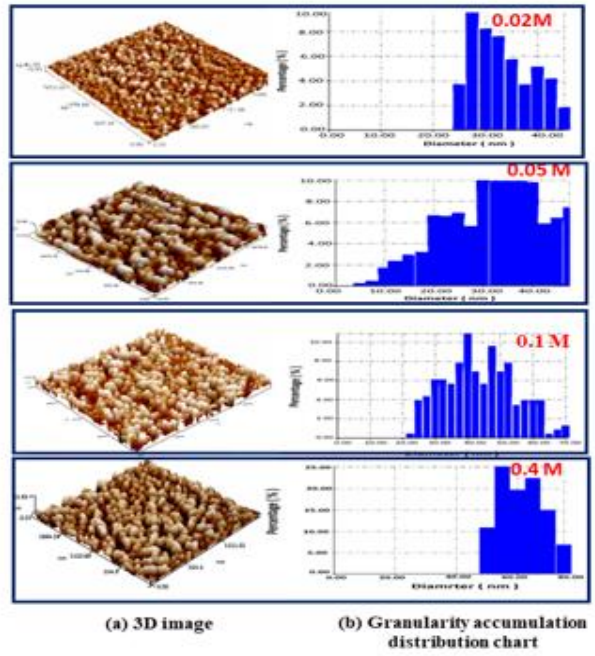

Figure 5. The AFM of CuO

Size and shape ZnO and CuO were described by the utilization of an electron emission-scanning microscopy ((FE-SEM) TESCAN, MIRA3, France). The SEM pictures of the nanoparticles appear in Figs. (7, 9) the morphology

arrangement of the nano oxide of numerous little nanoparticles, they look like a sphere,

Energy dispersive X-ray spectrometry (EDS) was used to utilize the chemical composite for each ZnO and CuO Depends on the atomic mass of the elements being detected was calculated by using the atomic percentage is the number of atoms of that element, at that weight percentage, divided by the total number of atoms in the sample multiplied by 100.

The (EDS) obtained for ZnO shown in the Fig. (6). Show Three main peak related to zinc with a dominant ratio were found alongside percent of oxygen peak, as shown in Table (5). Theoretical material ratio calculated for ZnO was 80.347, Zn % and 19.652, O%.

Table 5. Practical EDS percentage of ZnO

Sample		EDS	
No.	Conc.	Zn %	O%
1	0.02M	86.3	13.7
2	0.05M	85.5	14.5
3	0.1M	82.34	17.66
4	0.4M	84.23	15.77

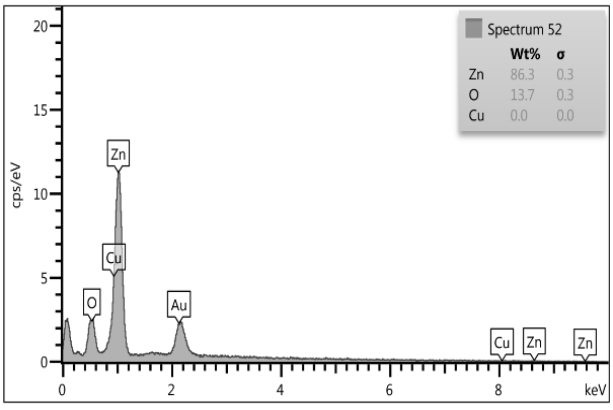

Figure 6. The EDS of 0.02 M ZnO

As comparison the peak values that calculated theoretical with values of EDS from SEM shown in table (5) was very close to calculated values that enhances the preparation results for ZnO nanoparticle (31) SEM images show that the ZnO with an average size that varies from (40- 80) nm for concentration from (0.02-0.4)M.

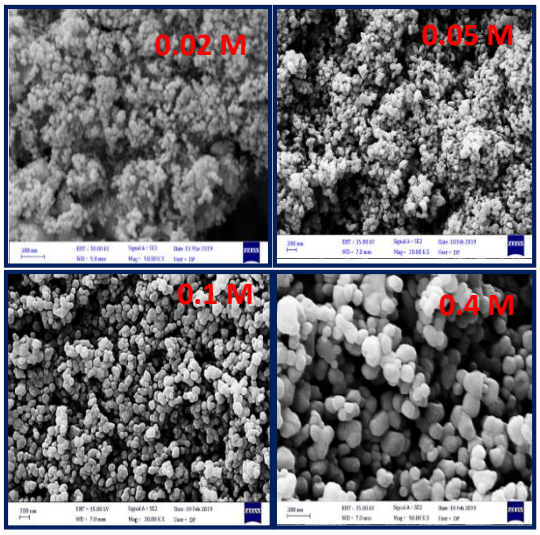

Figure 7. The SEM of ZnO

for CuO NPs in comparison, the practical values of CuO EDS with calculated 79.89 Cu% , 20.11, O% strengthen the prepared nano formula as show in table (6) is correct corresponds to the nano CuO that agreed with the literature (32).

Table 6. The practical EDS percentage of CuO

Sample		EDS	
No.	Conc.	Cu %	O%
1	0.02M	83.6	16.4
2	0.05M	80.5	19.5
3	0.1M	84.3	15.7
4	0.4M	82.9	17.1

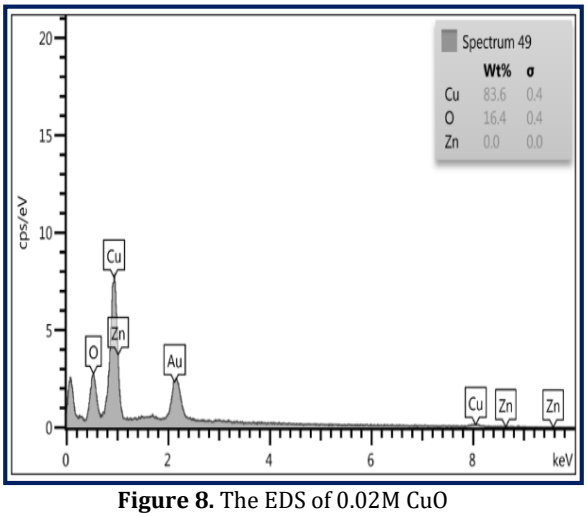

Figure 8. The EDS of 0.02M CuO

SEM images of the CuO NPs are shown in the fig. (9). as can be seen, the average particle size of CuO is about (35-50) nm, the nanoparticles have a good homogeneity, a spherical shape and an Appropriate separation. However, tine aggregates have also been observed because PVP used during the growing of nano that work as surfactant agent that aggregates due to highly activated copper to react due to its electronic d orbital, the particle size estimated from the SEM analysis is in good agreement with the XDR data. This small difference can be explained by the global vision represented by the XRD and the local characteristics demonstrated by SEM analysis that agree with the literature (33).

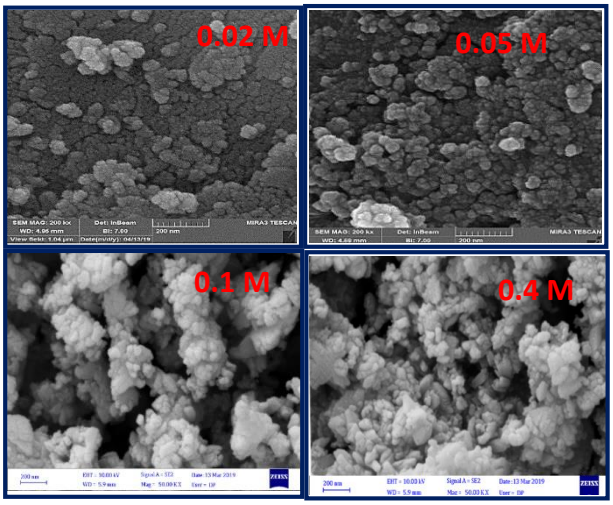

Figure 9. the SEM of CuO

Antibacterial test

Dissolving (28) g of nutrient agar into each (1000) ml of distilled water in a flask formed the agar medium. At (121) C° for (15) minutes, the agar medium was sterile by autoclave and poured into a Growth medium close the burner in a laminar airflow chamber. Then kept this to form a gel for 24 hours. Almost every microorganism completely immersed in pure liquid hot broth using a wire loop and therefore the flasks certainly kept for 24 hours in an incubator to enhance microorganisms of growth. The various concentrations of zinc oxide nanoparticles were put on growth dish (34), ZnO used with different concentrations in five dishes the Images bellow showed the inhibition zone,

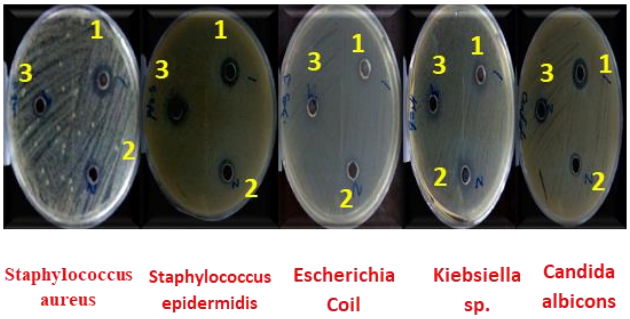

Images 1. the inhibition zone for ZnO with different concentration where
1 = 0.1 M, 2 = 0.02 M, 3 = 0.05 M.

From the antibacterial dish, the growth of selected bacteria can be explained by the above predominates describing that ZnO is more active in highly concentrated and effective areas more to inhibit the first two types of bacteria (Staphylococcus aureus and Staphylococcus epidermidis). Which is gram positive as a result, as can see in table (7). Nano ZnO can be used to effectively treat skin diseases(35).

Table 7. types of bacteria, fungi and inhibition zones with different concentration of nano ZnO

	Types of bacteria and fungi	Inhibition Zone (mm)			
		ZnO 0.4	ZnO 0.1	ZnO 0.05	ZnO 0.02
1	Staphylococcus aurous	22	13	----	----
2	Staphylococcus epidermidis	30	12	11	9
3	Escherichia coil	14	13	10	----
4	Klebsiella spp	11	12	11	11
5	Candida albicans	16	16	10	10

For CuO the growth of bacteria selected in the images (2). describing the behavior of CuO, can be explained by the fact that the sample is much more influential in areas of high concentration CuO and more effective for bacterial inhibition type Staphylococcus Aurous and Staphylococcus epidermidis which gram positive and Escherichia coli as gram negative so CuO can considered as active antibacterial agent (36,37) as showed in table (8) inhibition zones for CuO.

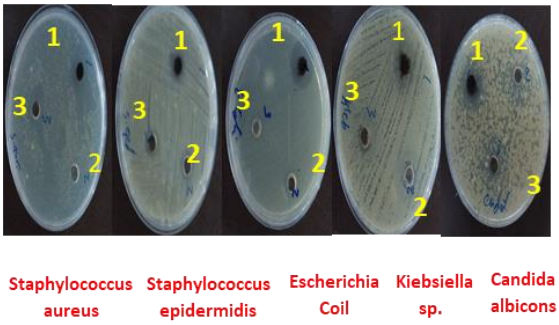

Images 2. the inhibition zone for CuO with different concentration where
1 = 0.1 M, 2 = 0.02 M ,3 = 0.05 M.

Table 8. Types of bacteria, fungi and inhibition zones with different concentration of nano CuO.

	Types of bacteria and fungi	Inhibition Zone (mm)			
		CuO 0.4	CuO 0.1	CuO 0.05	CuO 0.02
1	Staphylococcus aurous	25	14	11	----
2	Staphylococcus epidermidis	20	9	----	----
3	Escherichia coil	13	18	----	----
4	Klebsiella spp	12	----	----	10
5	Candida albicans	21	15	11	----

Conclusion

The results of the characterization showed that the synthesized nano metal oxides were absent of impurities and exhibited a high degree of crystalline nature with well-indexed diffraction peaks to established and hypothesized patterns, Crystallites size from X-ray diffraction exhibits (20.18, -49.51), (13.56-26.92) nm. The average grain size from AFM shows (31.63-84.80), (32.34-60.23) nm while from SEM (40-80), (35-50) for (0.02-0.4) M. The simple synthesized particles obtained optical properties with particle size below 100 nm, which categorizes them as nanoparticles, conforming to their established kinds. Copper oxide and zinc oxide may inhibit the concentration-dependent behavior of the bacteria. The highest rate of inhibition of zinc oxide is 30 mm for (Staphylococcus epidermidis)Whereas CuO nanoparticles show relatively less germicidal activity about 20mm. The nano arranged to be the nearest size to one another, in this manner, the high focus is progressively viable as antibacterial, On the other hand, unique molecule sizes show the capacity of these particles to lessen development paces of a few pathogenic microscopic organisms

REFERNCES

1. Qiu, S., Zhou, H., Shen, Z., Hao, L., Chen, H., & Zhou, X. (2020). Synthesis, characterization, and comparison of antibacterial effects and elucidating the mechanism of ZnO, CuO and CuZnO nanoparticles supported on mesoporous silica SBA-3. *RSC Advances*, *10*(5), 2767-2785. https://doi.org/10.1039/C9RA09829A
2. Ismail AH, Al-Bairmani HK, Abbas ZS, Rheima AM. Nanoscale Synthesis of Metal (II) Theophylline Complexes and Assessment of Their Biological Activity. Nano Biomed. Eng. 2020;12(2):139-47.
3. Rheima, A. M., Mohammed, M. A., Jaber, S. H., & Hameed, S. A. (2019). Synthesis of silver nanoparticles using the UV-irradiation technique in an antibacterial application. *Journal of Southwest JiaotongUniversity*, *54*(5). https://doi.org/10.35741/issn.02582724.54.5.34
4. Mohammed, M. A., Rheima, A. M., Jaber, S. H., & Hameed, S. A. (2020). The removal of zinc ions from their aqueous solutions by Cr2O3 nanoparticles synthesized via the UV-irradiation method. *Egyptian Journal of Chemistry*, *63*(2), 425-431. https://dx.doi.org/10.21608/ejchem.2019.17003.2042
5. Rheima, A. M., Mohammed, M. A., Jaber, S. H., & Hasan, M. H. (2019). Inhibition effect of silver-calcium nanocomposite on alanine transaminase enzyme activity in human serum of Iraqi patients with chronic liver disease. *Drug Invention Today*, *12*(11), 2818-2821.
6. Ali, A. A., Al-Hassani, R. M., Hussain, D. H., Rheima, A. M., & Meteab, H. S. (2020). Synthesis, spectroscopic, characterization, pharmacological evaluation, and cytotoxicity assays of novel nano and micro scale of copper (II) complexes against human breast cancer cells. *Drug Invention Today*, *14*(1).
7. Hussain, D. H., Rheima, A. M., Jaber, S. H., & Kadhim, M. M. (2020). Cadmium ions pollution treatments in aqueous solution using electrochemically synthesized gamma aluminum oxide nanoparticles with DFT study. *Egyptian Journal of Chemistry*, *63*(2), 417-424. https://dx.doi.org/10.21608/ejchem.2019.16882.2026
8. Ali, A. A., Al-Hassani, R. M., Hussain, D. H., Rheima, A. M., Abd, A. N., & Meteab, H. S. (2019). Fabrication of Solar Cells Using Novel Micro-and Nano-Complexes of Triazole Schiff Base Derivatives. *Journal of Southwest Jiaotong University*, *54*(6). https://doi.org/10.35741/issn.02582724.54.6.13
9. Hussain, D. H., Abdulah, H. I., & Rheima, A. M. (2016). Synthesis and Characterization of ɣ-Fe2O3 Nanoparticles Photo Anode by Novel Method for Dye Sensitized Solar Cell. *International Journal of Scientific and Research Publications*, *6*(10), 26-31.
10. Jabber, S. H., Hussain, D. H., Rheima, A. M., & Faraj, M. (2019). Comparing study of CuO synthesized by biological and electrochemical methods for biological activity. *Al-Mustansiriyah Journal of Science*, *30*(1), 94-98.
11. Ismail AH, Al-Bairmani HK, Abbas ZS, Rheima AM. Synthesis, characterization, spectroscopic, and biological activity studies of Nano scale Zn(II), Mn (II) and Fe (II) theophylline complexes. Journal of Xi'an University of Architecture & Technology. 2020; XII (II): 2775-2789.
12. Ali, A. A., Al-Hassani, R. M., Hussain, D. H., Rheima, A. M., Abd, A. N., & Meteab, H. S. (2019). Fabrication of Solar Cells Using Novel Micro-and Nano-Complexes of Triazole Schiff Base Derivatives. *Journal of Southwest Jiaotong University*, *54*(6). https://doi.org/10.35741/issn.02582724.54.6.13
13. Rheima, A. M., Hussain, D. H., & Abdulah, H. I. (2016). Silver nanoparticles: Synthesis, characterization and their used a counter electrodes in novel dye sensitizer solar cell. *IOSR Journal of Applied Chemistry*, *9*(10), 6-9. https://doi.org/10.9790/5736-0910010609
14. Zhao, X., Zhao, H., Yan, L., Li, N., Shi, J., & Jiang, C. (2020). Recent developments in detection using noble metal nanoparticles. *Critical Reviews in Analytical Chemistry*, *50*(2), 97-110. https://doi.org/10.1080/10408347.2019.1576496

15. Deng, Y., Handoko, A. D., Du, Y., Xi, S., & Yeo, B. S. (2016). In situ Raman spectroscopy of copper and copper oxide surfaces during electrochemical oxygen evolution reaction: identification of CuIII oxides as catalytically active species. *ACS Catalysis*, *6*(4), 2473-2481. https://doi.org/10.1021/acscatal.6b00205
16. Hashmi, M., Ullah, S., & Kim, I. S. (2019). Copper oxide (CuO) loaded polyacrylonitrile (PAN) nanofiber membranes for antimicrobial breath mask applications. *Current Research in Biotechnology*, *1*, 1-10. https://doi.org/10.1016/j.crbiot.2019.07.001
17. Velsankar, K., Sudhahar, S., Parvathy, G., & Kaliammal, R. (2020). Effect of cytotoxicity and aAntibacterial activity of biosynthesis of ZnO hexagonal shaped nanoparticles by Echinochloa frumentacea grains extract as a reducing agent. *Materials Chemistry and Physics*, *239*, 121976. https://doi.org/10.1016/j.matchemphys.2019.121976
18. Rosendo, F. R., Pinto, L. I., de Lima, I. S., Trigueiro, P., Honório, L. M. D. C., Fonseca, M. G., ... & Osajima, J. A. (2020). Antimicrobial efficacy of building material based on ZnO/palygorskite against Gram-negative and Gram-positive bacteria. *Applied Clay Science*, *188*, 105499. https://doi.org/10.1016/j.clay.2020.105499
19. Kumar, S. V., Bafana, A. P., Pawar, P., Faltane, M., Rahman, A., Dahoumane, S. A., ... & Jeffryes, C. S. (2019). Optimized production of antibacterial copper oxide nanoparticles in a microwave-assisted synthesis reaction using response surface methodology. *Colloids and Surfaces A: Physicochemical and Engineering Aspects*, *573*, 170-178. https://doi.org/10.1016/j.colsurfa.2019.04.063
20. Zare, M., Namratha, K., Byrappa, K., Surendra, D. M., Yallappa, S., & Hungund, B. (2018). Surfactant assisted solvothermal synthesis of ZnO nanoparticles and study of their antimicrobial and antioxidant properties. *Journal of materials science & technology*, *34*(6), 1035-1043. https://doi.org/10.1016/j.jmst.2017.09.014
21. Saleh, T. A., Fadillah, G., & Saputra, O. A. (2019). Nanoparticles as components of electrochemical sensing platforms for the detection of petroleum pollutants: A review. *TrAC Trends in Analytical Chemistry*, *118*, 194-206. https://doi.org/10.1016/j.trac.2019.05.045
22. Asamoah, R. B., Yaya, A., Mensah, B., Nbalayim, P., Apalangya, V., Bensah, Y. D., ... & Annan, E. (2020). Synthesis and characterization of zinc and copper oxide nanoparticles and their antibacteria activity. *Results in Materials*, 100099. https://doi.org/10.1016/j.rinma.2020.100099
23. Escobedo-Morales, A., Ruiz-López, I. I., Ruiz-Peralta, M. D., Tepech-Carrillo, L., Sánchez-Cantú, M., & Moreno-Orea, J. E. (2019). Automated method for the determination of the band gap energy of pure and mixed powder samples using diffuse reflectance spectroscopy. *Heliyon*, *5*(4), e01505. https://doi.org/10.1016/j.heliyon.2019.e01505
24. Matysiak, W., Tański, T., & Zaborowska, M. (2019). Manufacturing process and characterization of electrospun PVP/ZnO NPs nanofibers. *Bulletin of the Polish Academy of Sciences. Technical Sciences*, *67*(2). http://dx.doi.org/10.24425/bpas.2019.128601
25. Kamila, S., & Venugopal, V. R. (2017). Synthesis and structural analysis of different CuO nano particles. *Int. J. Appl. Sci. Eng*, *14*, 133-146. http://dx.doi.org/10.6703/IJASE.2017.14(3).133
26. Kumar, S. S., Venkateswarlu, P., Rao, V. R., & Rao, G. N. (2013). Synthesis, characterization and optical properties of zinc oxide nanoparticles. *International Nano Letters*, *3*(1), 30. https://doi.org/10.1186/2228-5326-3-30
27. Goswami, M., Adhikary, N. C., & Bhattacharjee, S. (2018). Effect of annealing temperatures on the structural and optical properties of zinc oxide nanoparticles prepared by chemical precipitation method. *Optik*, *158*, 1006-1015. https://doi.org/10.1016/j.ijleo.2017.12.174
28. Tamaekong, N., Liewhiran, C., & Phanichphant, S. (2014). Synthesis of thermally spherical CuO nanoparticles. *Journal of Nanomaterials*, *2014*. https://doi.org/10.1155/2014/507978
29. Davarpanah, S. J., Karimian, R., & Piri, F. (2015). Synthesis of copper (II) oxide (CuO) nanoparticles and its application as gas sensor. *Journal of Applied Biotechnology Reports*, *2*(4), 329-332.
30. Levkevich, E. A., Yukhnovets, O., Moshnikov, V. A., & Maximov, A. I. (2019, January). Photocatalytic Properties of ZnO/CuO Heterostructures. In *2019 IEEE Conference of Russian Young Researchers in Electrical and Electronic Engineering (EIConRus)* (pp. 777-779). IEEE. https://doi.org/10.1109/EIConRus.2019.8657316
31. Vasile, E., Plugaru, R., Mihaiu, S., & Toader, A. (2011). Study of microstructure and elemental micro-composition of ZnO: Al thin films by scanning and high resolution transmission electron microscopy and energy dispersive X-ray spectroscopy. *Romanian Journal of Information Science and Technology*, *14*(4), 346-355.
32. Deki, S., Akamatsu, K., Yano, T., Mizuhata, M., & Kajinami, A. (1998). Preparation and characterization of copper (I) oxide nanoparticles dispersed in a polymer matrix. *Journal of Materials Chemistry*, *8*(8), 1865-1868. https://doi.org/10.1039/A801506F
33. Sahooli, M., Sabbaghi, S., & Saboori, R. (2012). Synthesis and characterization of mono sized CuO nanoparticles. *Materials Letters*, *81*, 169-172. https://doi.org/10.1016/j.matlet.2012.04.148
34. Zhang, L., Jiang, Y., Ding, Y., Povey, M., & York, D. (2007). Investigation into the antibacterial behaviour of suspensions of ZnO nanoparticles (ZnO nanofluids). *Journal of Nanoparticle Research*, *9*(3), 479-489. https://doi.org/10.1007/s11051-006-9150-1
35. Vieira, C. O., Grice, J. E., Roberts, M. S., Haridass, I. N., Duque, M. D., Lopes, P. S., ... & Martins, T. S. (2019). ZnO: SBA-15 nanocomposites for potential use in sunscreen: preparation, properties, human skin penetration and toxicity. *Skin pharmacology and physiology*, *32*(1), 32-42. https://doi.org/10.1159/000491758
36. Niaz, N., Bano, A., Fasim, F., Kausar, R., Khan, B. A., Zafar, N., ... & Uzair, B. (2018). Synthesis, characterization and evaluation of antibacterial activity of copper oxide nanoparticles against clinical strains of Staphylococcus aureus. *Pakistan journal of pharmaceutical sciences*, *31*.
37. Azam, A., Ahmed, A. S., Oves, M., Khan, M. S., Habib, S. S., & Memic, A. (2012). Antimicrobial activity of metal oxide nanoparticles against Gram-positive and Gram-negative bacteria: a comparative study. *International journal of nanomedicine*, *7*, 6003. https://dx.doi.org/10.2147%2FIJN.S35347